Desalination and Water Treatment
www.deswater.com

doi: 10.5004/dwt.2021.27537

233 (2021) 133–149
September

Kinetics and thermodynamics of removal of metal ions using EDTA-modified cation ion exchange resin

Smita N. Katariya, Sanjeev Kumar, Ran Bahadur Yadav*

Applied Chemistry Department, Faculty of Technology and Engineering, The Maharaja Sayajirao University of Baroda, Vadodara - 390001, Gujarat, India, Tel. +91 9408091499; email: rbyadavmsu@gmail.com (R.B. Yadav), Tel. +91 8866225394; email: simsk1896@gmail.com (S.N. Katariya), Tel. +91 9427453243; email: drksanjeev@gmail.com (S. Kumar)

Received 2 January 2021; Accepted 24 June 2021

ABSTRACT

Amberlite IRA-400(Cl^-) (polymeric resin) has been modified with disodium salt of ethylenediaminetetraaceticacid (Na_2EDTA). The modified chelating resin (MCR) has been characterized by energy-dispersive X-ray spectroscopy, scanning electron microscopy and Fourier transform infrared spectroscopy techniques. Distribution coefficient (K_d) has been determined with MCR for various metal ions (Co^{2+}, Ni^{2+}, Cu^{2+}, Zn^{2+}, Cd^{2+}, Hg^{2+}, Pb^{2+}) and K_d data have been analysed using Langmuir and Freundlich adsorption isotherms. Thermodynamic parameters, (equilibrium constant, standard Gibbs free energy, enthalpy and entropy changes), using various chemical kinetics model (pseudo-first-order, pseudo-second-order or intra-particle), have been computed by performing metal ion exchange at different temperatures (299, 309, 319 and 329 K). Elution behaviors of above metal ions have been observed using various electrolytes (NH_4NO_3, HNO_3, $HClO_4$, CH_3COOH). It has been found that exchange process follows Langmuir adsorption isotherm together with second order kinetic model.

Keywords: Transition metal ions; Heavy metal ions; Sorption; Modified chelating resin; Langmuir isotherm

1. Introduction

Aqueous bodies are most valuable and essential components on the earth. Due to unique nature, water is required for various vital activities of living systems. Also, it plays important role in industries because of its abundance and solvent property. Unfortunately, quality of water resources is deteriorating day by day due to growth in population/civilization, domestic sewage, agricultural activities, industrialization, geological and climate changes [1–4]. The important environmental issue for water pollution is the presence of heavy metal ions coming from various sources. Many heavy metals are highly toxic (cobalt, nickel, copper, zinc, cadmium, mercury and lead). These metal ions are chemically and biologically non-degradable and are toxic even at very low concentrations [5–8]. Various industries such as mechanical, metallurgical, mining, pigment, paper, etc, release wastewater containing metal or metal derivatives [9–12]. Above toxic metal ions remain one of the serious public health problems for human health. Heavy metal toxicity can cause hypertension, nephritis, abdominal pain, vomiting, anaemia, brain diseases, high blood pressure, genetic defect and lung cancer [13–17]. Recently, different methods are adopted for treating waste water [18–20]. Different methodologies (precipitation, adsorption, electroplating,

* Corresponding author.

ion exchange, membrane separation, flotation and reverse osmosis) are available for the removal of heavy metal ions from aqueous discharge [21–26]. Among various processes, ion exchange is one of the most effective and simple available process for the removal of transition and heavy metal ions from waste water [27,28]. An extensive literature is available on types of adsorbents (activated carbons [29–31], surface modified zeolites [32,33], graphene oxide and its composites [34], biosorbents [35–38], tetravalent metal phosphonate [39] and chelating materials [40,41]) utilised for the removal of metal ions. A few studies, using ion exchange resins such as Dowex A-1, Duolite GT-73, Amberlite 252 ZU, Amberlite IR-120, Amberlite IRA-68, Amberlite IRA-743, and Amberlite IRC-718, Lewatit TP 207, Lewatit CNP 80, and Amberlite IRA-420, have also been reported [42–45].

The exchange/adsorption property of the adsorbents depends upon the functional groups present on their surfaces [46]. Functional groups such as carboxylic [47,48], phenolic, amide and amine [49] provide binding sites for metal ions. The donor atom of functional groups behaves as Lewis base, which forms co-ordinate bond with heavy metal ion, which acts as Lewis acid [16]. However, polymeric resin has not been modified with the point of view of insertion of chelating capacity in the resin, which can potentially be used for binding/exchange of metal ions.

The aim of the work is to examine the removal of metal ions by using commercially available polymeric resin (Amberlite IRA-400(Cl^-)). In the present study, the resin has been modified with disodium salt of ethylenediaminetetraacetic acid (Na_2EDTA). This modification inserts chelating characteristics in the above polymeric resin (modified chelating resin, MCR), which may be used to bind metal ions from external matrices. MCR may show chelating properties due to presence of two –COOH groups and two >N- groups. –COOH groups are responsible for exchange of metal ions with H^+ of carboxylic group and simultaneously imine groups bind with metal ions [Transition metal (Co^{2+}, Ni^{2+}, Cu^{2+}, Zn^{2+}) and heavy metal (Cd^{2+}, Hg^{2+}, Pb^{2+})] through co-ordinate bonds. Na_2EDTA behaves as tetra dentate chelating ligand. This incorporates effect of complexing agent in the MCR and responsible for separating metal ions from background solution [17]. The MCR was characterized by energy-dispersive X-ray spectroscopy (EDX), scanning electron microscopy (SEM), and Fourier transform infrared spectroscopy (FTIR). In aqueous and various electrolyte media/concentration, distribution coefficients (K_d) of metal ions [Transition metal (Co^{2+}, Ni^{2+}, Cu^{2+}, Zn^{2+}) and heavy metal (Cd^{2+}, Hg^{2+}, Pb^{2+})] have been computed by batch equilibrium technique. Effect of pH has also been seen on the exchange process. The Langmuir and Freundlich adsorption models have been applied at various fixed temperatures and different concentrations of the exchanging metal ions. Thermodynamic parameters, equilibrium constant (K), standard Gibbs free energy ($\Delta G°$), enthalpy ($\Delta H°$), and entropy ($\Delta S°$) changes, were evaluated by temperature dependence of the exchange process. Kinetic study, for exchange of metal ion, was performed to obtain information related to mode of kinetic exchange. Elution behavior of above metal ions has also been seen using various acids and electrolyte by adopting column method.

2. Experimental section

2.1. Starting materials

Amberlite IRA-400(Cl^-) resin (purchased from Merck India), disodium salt of ethyelenediaminetetra aceticacid (Na_2EDTA, M_w = 372.24 g/mol) (from BIRCH), and all metal salts indicators (from S d fine-chem. limited and Loba-chem limited). Glassware were washed, cleaned and rinsed with dilute hydro chloric acid, distilled water and de-ionized water (D/W), respectively. The pH adjustments were made (from pH 1 to pH 7) using nitric acid (M_w = 63.01 g/mol), sulphuric acid (M_w = 98.07 g/mol) and sodium hydroxide (M_w = 40.00 g/mol) solutions as per the requirement. All reagents used in the present work were of analytical grade and solutions were prepared in de-ionized water.

2.2. Modification of Amberlite IRA-400(Cl^-) resin

MCR was prepared by treating 100 g of Amberlite IRA-400(Cl^-) resin with 1,000 mL of aqueous solution of 0.01 M (Na_2EDTA) solution in a round bottom flask. Contents of flask were left for 24 h with constant shaking to ensure the complete modification. The MCR was separated from the aqueous solution and washed several times with de-ionized water until the supernatant liquid was found free from chloride ion, the resin was dried in an electric oven (60°C).

2.3. Physical measurements

The morphological changes of the samples, Amberlite IRA-400(Cl^-) resin and MCR, were analyzed using SEM. The FTIR spectra were recorded (in the form of KBr pellets) on Shimadzu-8400s. SEM and EDX of the samples were taken by using EDX OXFORD 6587 while pH of the samples was measured using ANALAB (Vadodara, India), pH meter. For thermodynamic and kinetic studies, an electric, temperature-controlled shaker bath having a temperature variation of ±0.5°C was used.

2.4. Distribution study

The distribution coefficient (K_d) was evaluated by batch method for the transition and heavy metal ions (Co^{2+}, Ni^{2+}, Cu^{2+}, Zn^{2+}, Cd^{2+}, Hg^{2+} and Pb^{2+}) by taking 0.1 g of the MCR, equilibrated with 10 mL of 0.001 M to 0.007 M of all metal solutions (for different durations (15, 30, 45, 60, 75, 90, 105, 120, 135, 150 min and upto 24 h)) at room temperature. Concentration of the metal ion was determined by using complexometry titration before and after sorption on the MCR.

The K_d value was also evaluated at optimum condition with 0.1 g of the exchanger in aqueous as well as in presence of various electrolytic media [nitric acid (HNO_3), perchloric acid ($HClO_4$), acetic acid (CH_3COOH), ammonium nitrate (NH_4NO_3)] for two different metal concentrations (0.02 and 0.2 M) at room temperature. K_d values have been calculated using Eq. (1) [50].

$$\left[K_d = \frac{(I-F)}{F} \times \frac{V}{W}\right] \quad (1)$$

where I is the initial [metal ion] solution, F is the final [metal ion] solution, W is the weight of the exchanger in gram and V is the volume of the metal ion solution in mL.

2.5. Adsorption studies

2.5.1. Effect of pH, contact time and temperature on adsorption/ion exchange

Adsorption of transition and heavy metal ions (Co^{2+}, Ni^{2+}, Cu^{2+}, Zn^{2+}, Cd^{2+}, Hg^{2+} and Pb^{2+}) has been carried out by MCR shaking 0.1 g MCR with 10 mL of 0.002 M metal ion solution under adjusted pH (1–7) by using pH meter. The decanted solution was used to determine quantity of the transition and heavy metal ion by complexometry titrations [51]. The percentage uptake was calculated using the following expression:

$$\left[\frac{(C_0 - C_e)}{C_0}\right] \times 100 \quad (2)$$

where C_0 and C_e are the initial and final concentrations of metal ion in mg/L, respectively. This experiment was performed in a temperature range of 299–329 K with a 10-K interval.

2.6. Thermodynamic studies

2.6.1. Equilibrium time determination

It is determined with 0.1 g of MCR, which was shaken with 10 mL of 0.002 M metal ion solution in a stoppered conical flask (varying time from 15 min to 24 h). After each time interval, the mixture was decanted and the metal ion concentration in the solution was determined by complexometry titration. A plot of the fractional attainment of equilibrium ($U(t)$) vs. time (t) for exchanged metal. This shows that an equilibrium has been attained within 120 min (optimum equilibrium time).

2.6.2. Equilibrium experiments

In these experiments, 0.1 g of MCR, at different temperatures (299–329 K with a 10 K interval), shaked with 20 mL of a mixture of solution (containing 0.06 M HCl and 0.02 M metal ion solution (1, 3, 5, …, 19 mL of 0.02 M metal ion solution and 19, 17, 15, …, 1 mL of 0.06 M HCl), After each time interval, metal ion concentration was determined by complexometry titration. Temperature dependent data have been used to obtain thermodynamic parameters such as equilibrium constant (K), standard Gibbs free energy ($\Delta G°$), entropy ($\Delta S°$) and enthalpy ($\Delta H°$) changes [52].

2.7. Sorption kinetics

The kinetics of sorption of MCR was investigated using the pseudo-first-order, pseudo-second-order and intraparticle diffusion reaction models.

2.7.1. Pseudo-first-order kinetic model

The kinetic model can be given by Eq. (3) [53]:

$$\log(q_e - q_t) = \log q_e - \left(\frac{K_1}{2.303}\right)t \quad (3)$$

where q_t and q_e are the amount of solute adsorbed per g of sorbent (mg/g) at certain time (t) and at equilibrium, respectively. K_1 is the rate constant of pseudo-first-order sorption (min^{-1}). The straight line plot of $\log(q_e - q_t)$ against t gives $\log(q_e)$ as slope and $K_1/2.303$ as intercept.

2.7.2. Pseudo-second-order kinetic model

The model is represented by Eq. (4) [54]:

$$\frac{t}{q_t} = \frac{1}{(K_2 q_e^2)} + \frac{t}{q_e} \quad (4)$$

where K_2 is the rate constant of pseudo-second-order sorption (g/mg min) and q_e values are calculated from the slope of the straight line. The plots of t/q_t vs. t (straight lines) the slope and intercept are $1/q_e$ and $1/K_2 q_e^2$, respectively.

2.7.3. Weber–Morris intraparticle diffusion model

The expression for the Weber–Morris intraparticle diffusion model is represented by Eq. (5) [55]:

$$q_t = K_{id} t^{\frac{1}{2}} + C \quad (5)$$

where K_{id} is the intraparticle diffusion rate constant (mg/g $min^{1/2}$) and C (mg/g) is the intercept. K_{id} can be obtained by the plot of q_t vs. $t^{1/2}$.

2.8. Elution studies

Elution studies were performed by taking 0.5 g of MCR in a column followed by washing with de-ionized water (flow rate 0.5 mL/min). Metal ion (Co^{2+}, Ni^{2+}, Cu^{2+}, Zn^{2+}, Cd^{2+}, Hg^{2+} and Pb^{2+}) has been determined quantitatively by complexometry titration. For such study (single metal), column was prepared. The metal ion solution (0.002 M, 10 mL) was loaded to the column. The metal ion loaded column was eluted with eluents such as HNO_3, $HClO_4$, CH_3COOH and NH_4NO_3 (0.02 M or 0.2 M). The % of metal ion eluted (% E) was calculated using Eq. (6).

$$\%E = \left(\frac{C_e}{C_0}\right) \times 100 \quad (6)$$

where C_e is the amount of metal ion in the eluted solution and C_0 is the amount of metal ion present in the loaded solution.

3. Result and discussion

Amberlite IRA-400(Cl^-) resin is a strongly basic, anion exchange resin. Chloride ion is associated with tertiary

nitrogen of amine group by electrostatic bond. When, Amberlite IRA-400(Cl^-) resin was shaked with 0.01 M solution of Na_2EDTA for 24 h. Chloride ion was completely substituted with $EDTA^{2-}$ and substitution of Cl^- was confirmed by EDX analysis. The resultant MCR was obtained as reddish brown translucent spherical beads or granules and insoluble in water. The MCR contains two nitrogen of amine group and two oxygen of carboxylic group, offering chelating sites to metal ion and behave as cation exchange unit. The structure of metal-loaded MCR has been shown in Fig. 1. Surface morphologies for pure and modified were investigated by SEM analysis (Fig. 2). This study shows that no significant modification in surface morphology takes place on the insertion of chelating moiety (i.e., Na_2EDTA). This reveals that chelating moiety binds at the surface of the resin and does not affect internal resin structure and hence morphology.

EDX spectra of Amberlite IRA-400(Cl^-) resin, MCR, transition metal (Zn^{2+}) loaded MCR and heavy metal (Pb^{2+}) loaded MCR are illustrated in Figs. 3a–d. Absence of Cl^- ion in the MCR indicates that Cl^- ion has been removed by $EDTA^{2-}$. Presence of Co^{2+}, Ni^{2+}, Cu^{2+}, Cd^{2+} and Hg^{2+} metal ions in the images of metal-loaded MCR and tables of EDX also revealed uptake of metal ions by modified resin as shown in Figs. S1 and S2.

FTIR absorption spectrum of sample Amberlite IRA-400(Cl^-) resin, modified Amberlite IRA-400(Cl^-) resin (MCR), and Pb^{2+} metal-loaded MCR is presented in Fig. S3. FTIR spectra show a broad bend in the 400–4,000 cm^{-1} range. A sharp medium band at 1,690 cm^{-1} is attributed to –C=O stretching vibrations in the modified Amberlite IRA-400(Cl^-) resin. It is a confirmation of the modification of Amberlite IRA-400(Cl^-) resin with disodium salt of EDTA. The absorption peak 1,690 cm^{-1} is also observed in metal-loaded MCR. The O–H bending vibration is observed at 1,408 cm^{-1} in MCR and it shifted to 1,411 cm^{-1} after metal-loaded MCR. The absorption peak observed at 1,220 cm^{-1} is due to (C–N) in MCR, which shifted to 1,232 cm^{-1} in metal-loaded MCR. The metal ion has positive character when it is attached with coordinating sites of modified resin and attracts electron density. So energy of bands are changed and small peaks get merged and converts into an intense band in FTIR spectrum (Fig. S3).

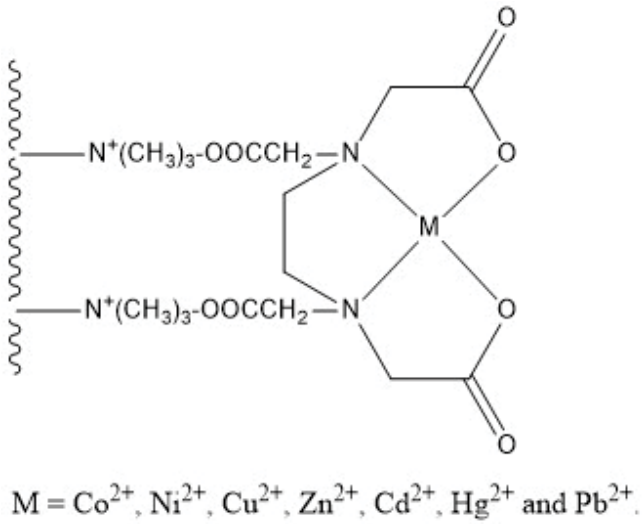

Fig. 1. Schematic structure of metal-loaded MCR.

3.1. Distribution studies

3.1.1. Distribution coefficient (K_d) of metal ion

Movement/exchange of a particular metal ion, towards an ion exchanger, has been found to be dependent on (1) ion exchanger nature, (2) nature of background medium and (3) size and hydration of the metal ion [39]. The present exchange process can be interpreted in the light of above factors. K_d values, evaluated for all metal ions towards MCR, have been compiled in Table 1 (and also in Fig. S4). It has been observed that K_d value increases (up to 0.002 M) and then decreases as the metal ion concentration increases in the background solution (>0.002 to 0.007 M). The initial K_d value increase in lower concentration range may be due to availability of more exchangeable sites and hence responsible for nearly complete exchange of metal ions. Sufficient sites are not available at higher metal ion concentrations and hence the observed K_d value decreases. High K_d values are observed in the aqueous media of Co^{2+} (0.72 Å) and Pb^{2+} (1.44 Å) metal ion. Comparison of K_d data (Table 2) with earlier studies [51,56,57], performed with other types (cerium phosphate and modified cellulose) of exchangers/adsorbents, shows that the present MCR distinctly better, which may be due to the insertion of chelating moiety, which facilitates metal binding.

K_d values determined for all metal ions under study, at optimum metal ion concentration (0.002 M) and in different electrolytic solutions (0.02 or 0.2 M), are given in Table 2. Further, K_d values in strong electrolytic media are lower as compared with weak electrolyte/aqueous media. The behavior is driven by increased ionic mobility and higher affinity of metal ion towards the exchanger compared with H^+ ions. It has been observed that the K_d values are lower in 0.2 M concentration of electrolyte, which can be understood in the light of competition between metal ion and electrolytic cation (H^+ or NH_4^+). Similar studies of metal ion exchange have also been performed with non-electrolyte (tert-butanol) [45]. In this study, K_d values were found to increase with increase in [(tert-butanol)] in the background solution. This suggests that nature and composition of electrolyte/non-electrolyte has a role to play in the mobility/exchange of metal ion towards exchanger.

3.2. Adsorption studies

3.2.1. Effect of pH and contact time on the adsorption of metal ions

It is known that pH of the solution affects the solubility of metal ion and the competition ability with hydrogen ions. The sorption of transition and heavy metal ions was carried out in the pH range of 1.0 to 7.0 and data are shown in Table 3. Sorption data of all metal ions, at various pH, are also presented in Fig. S5. It can be seen in Fig. S5 that % uptake of metal ions increases with increase in the solution pH. At lower pH, percentage uptake of metal ions is also

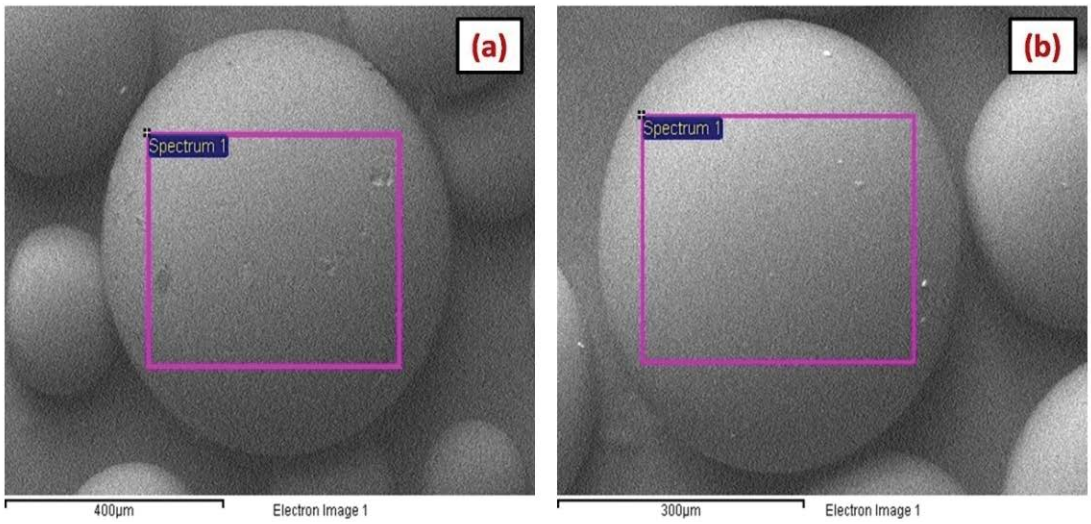

Fig. 2. SEM micrographs of (a) Amberlite IRA-400(Cl^-) resin and (b) MCR.

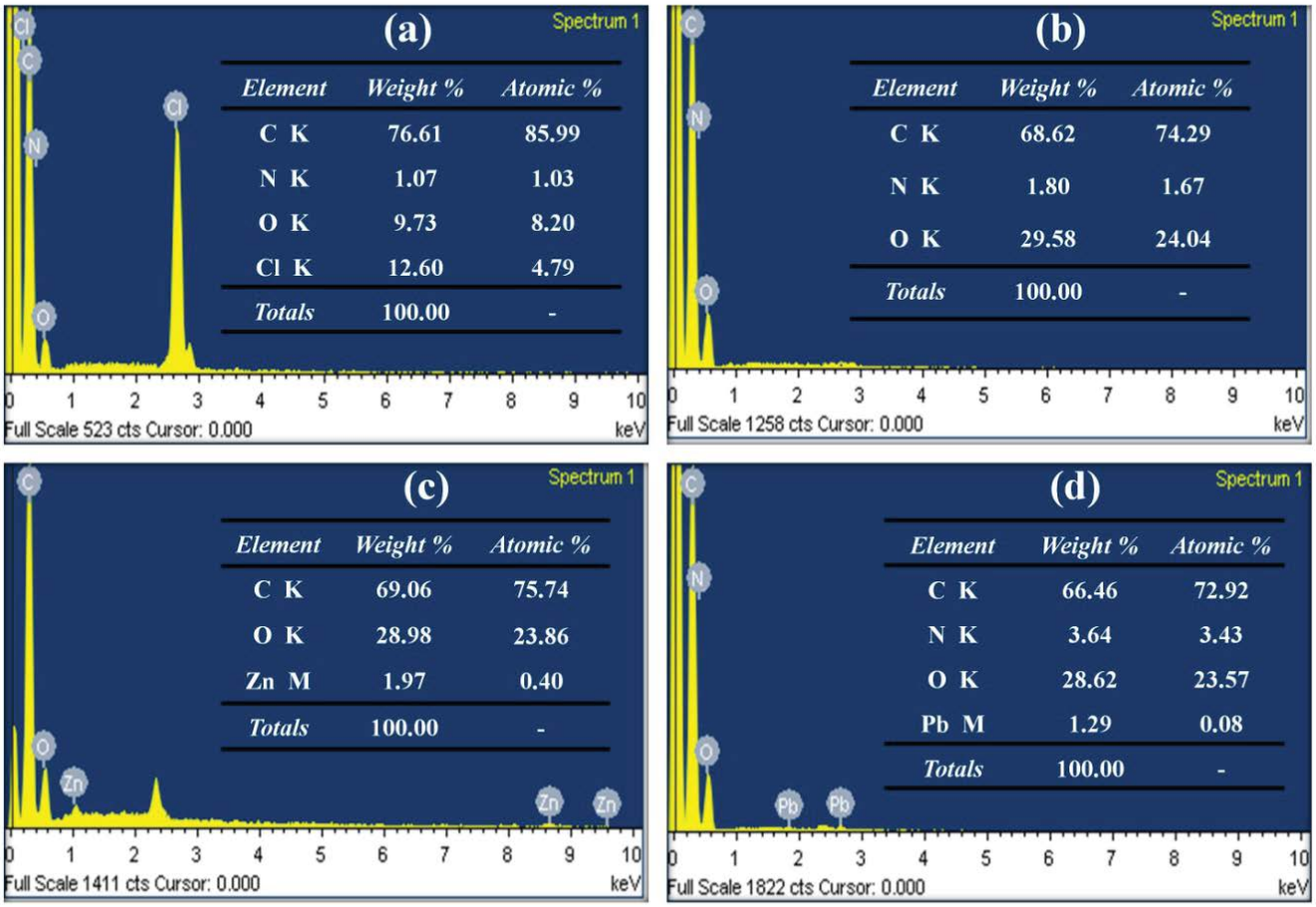

Fig. 3. EDX spectra of (a) Amberlite IRA-400(Cl^-) resin, (b) MCR, (c) Zn^{2+} loaded MCR and (d) Pb^{2+} loaded MCR.

lower. This is because of the hydrogen competition of H^+ and metal ions for sorption/exchange sites. Experiments were not extended to above pH 7.0 because due to precipitation of all metal ions in the form of their hydroxides.

Contact time is one of the important parameters, which affect the adsorption. K_d increases with time (up to 120 min) and then show no further increase till 24 h (Table 4). This implies that after saturation, it is difficult for the metal ion

Table 1
Distribution coefficient (K_d) values (mL/g) with varying transition and heavy metal ions for MCR

Metal ions	Ionic radii (Å)	Distribution coefficient (K_d) values (mL/g) at different concentrations (M)						
		0.001 M	0.002 M	0.003 M	0.004 M	0.005 M	0.006 M	0.007 M
Co^{2+}	0.72	164.7	212	128.81	105.55	91.66	64.7	39.13
Ni^{2+}	0.72	90.47	130.76	90.47	75	44.44	34.61	23.52
Cu^{2+}	0.74	104.54	122.22	80.55	45.45	34.86	34.4	28.57
Zn^{2+}	0.74	100	135.29	66.66	52.63	49.19	40	29.71
Cd^{2+}	0.97	114.28	214.81	100	64.70	50	42.85	38.46
Hg^{2+}	1.10	73.91	103.12	73.07	55.84	47.05	33.85	21.01
Pb^{2+}	1.44	133.33	341.17	91.66	63.15	43.93	39.88	36.58

Table 2
Distribution coefficient (K_d) values (mL/g) with different metal ions in various electrolyte media (0.02 or 0.2 M)

Metal ions	Aqueous media	K_d values (mL/g) at different concentrations (M) in different electrolytes							
		NH_4NO_3		HNO_3		$HClO_4$		CH_3COOH	
		0.02 M	0.2 M	0.02 M	0.2 M	0.02 M	0.2 M	0.02 M	0.2 M
Co^{2+}	212	89.65	83.33	93.54	66.66	170.83	160	150	122.22
Ni^{2+}	130.76	124	89.65	77.41	57.14	103.44	83.33	120	100
Cu^{2+}	122.22	83.33	78.51	87.5	77	89.65	78.57	106.89	103.70
Zn^{2+}	135.29	122.22	110.71	100	89.65	103.70	87.5	113.79	100
Cd^{2+}	214.81	170.83	140	103.12	100	130.76	122.22	132.14	124.13
Hg^{2+}	103.12	100	96.96	45.16	40.62	71.42	66.66	83.33	87.5
Pb^{2+}	341.17	293.33	292.85	120	108.33	172.72	150	313.33	300

Table 3
Percentage uptake of metal ions with varying pH using MCR

pH	Uptake of metal ion (%)						
	Co^{2+}	Ni^{2+}	Cu^{2+}	Zn^{2+}	Cd^{2+}	Hg^{2+}	Pb^{2+}
1	62.82	50	60	56.25	56.47	41.53	68
2	65.38	51.66	62.5	60	57.64	44.61	72
3	67.94	53.33	63.75	61.25	58.82	46.15	74.66
4	74.35	55	65	62.5	60	47.69	77.33
5	75.64	56.66	68.75	63.75	61.17	49.23	80
6	80.76	58.33	70	66.25	62.35	–	84
7	–	–	71.25	–	–	–	–

to adsorbed any more from the solution. This is due to the fact that initially maximum number of free sites are available (in the MCR) for adsorption of metal ions. However, occupancy of sites causes near saturation in ~120 min, (optimum time, see Fig. 5) and a level of effect [58].

3.3. Adsorption isotherms

Adsorption isotherms are a critical piece of information on optimization of the use of adsorbents. Adsorption equilibrium isotherms provide fundamental physico-chemical information to evaluate the applicability of the adsorption process [30]. The relationship between the quantities of the metal ions adsorbed and the concentration equilibrium (C_e) can be obtained using the linear form of the Langmuir and Freundlich isotherms (most commonly used adsorption isotherm models).

The equilibrium isotherm data of metal ion adsorption can be described by linearized Langmuir adsorption isotherm expression (Eq. (7)).

$$\frac{C_e}{(X/m)} = \frac{1}{(bV_m)} + \frac{C_e}{V_m} \tag{7}$$

where C_e (mg/g) is the amount of adsorbate adsorbed (at the equilibrium), X is the equilibrium concentration of adsorbate, m is the amount of adsorbent, while X/m represents q_e. V_m (mg/g) is the maximum monolayer adsorption capacity and b (dm^3/mg) is the Langmuir constant related to energy of adsorption and the affinity of the binding sites. A linear model of Langmuir isotherm was drawn by plotting C_e/q_e (g/L) vs. C_e (mg/L). These plots (with good correlation coefficient, R^2) result Langmuir constants, V_m and b (dimensionless). Langmuir constants, V_m and b (dimensionless), Table 5 contains data for transition metal and heavy metal ions. Figs. 4a and b show representative plots for Co^{2+} and Pb^{2+} and data for other metal ions are shown in Figs. S6 and S7. The separation factor R_L, used to predict favorability of the adsorption process, was calculated using the expression (Eq. (8)).

Table 4
Effect of contact time on K_d value of metal ions using MCR

	Equilibrium values (mequie/g)									
Metal ions	15 min	30 min	45 min	60 min	75 min	90 min	105 min	120 min	135 min	150 min
Co^{2+}	0.86792	0.90566	0.92453	0.94340	0.95283	0.96226	0.97170	1	1	1
Ni^{2+}	0.73529	0.76471	0.77941	0.79412	0.82353	0.88235	0.94118	1	1	1
Cu^{2+}	0.77273	0.79545	0.84091	0.90909	0.93182	0.95455	0.97727	1	1	1
Zn^{2+}	0.88889	0.91111	0.92222	0.93333	0.95333	0.95556	0.97778	1	1	1
Cd^{2+}	0.89655	0.93103	0.93276	0.94828	0.95862	0.96552	0.98276	1	1	1
Hg^{2+}	0.87879	0.90909	0.92121	0.93939	0.95455	0.96970	0.98485	1	1	1
Pb^{2+}	0.70690	0.74138	0.75862	0.77586	0.81034	0.86207	0.94828	1	1	1

Table 5
Langmuir constants evaluated for transition and heavy metal ions using MCR

		Langmuir constants			
Metal ions	Temperature (K)	R^2	b (dm^3/mg)	V_m (mg/g)	R_L
Co^{2+}	299	0.997	0.0043	21.27	0.945
	309	0.998	0.0048	20.83	0.939
	319	0.999	0.0048	21.27	0.939
	329	0.998	0.0051	21.27	0.936
Ni^{2+}	299	0.996	0.0050	25.64	0.941
	309	0.997	0.0063	25.00	0.927
	319	0.985	0.0079	25.00	0.910
	329	0.971	0.0090	25.00	0.899
Cu^{2+}	299	0.948	0.0043	20.00	0.949
	309	0.945	0.0051	20.00	0.940
	319	0.942	0.0064	19.60	0.926
	329	0.986	00077	19.60	0.912
Zn^{2+}	299	0.981	0.0025	27.02	0.969
	309	0.987	0.0036	24.39	0.956
	319	0.997	0.0044	25.00	0.947
	329	0.996	0.0057	23.80	0.932
Cd^{2+}	299	0.997	0.0024	43.47	0.970
	309	0.998	0.0026	45.45	0.968
	319	0.999	0.0025	47.61	0.969
	329	0.999	0.0028	47.61	0.966
Hg^{2+}	299	0.957	0.0019	35.71	0.976
	309	0.963	0.0022	35.71	0.973
	319	0.968	0.0024	37.03	0.970
	329	0.972	0.0027	37.03	0.967
Pb^{2+}	299	0.999	0.0032	58.82	0.964
	309	0.997	0.0060	55.55	0.935
	319	0.997	0.0080	55.55	0.915
	329	0.993	0.0142	55.55	0.859

$$R_L = \frac{1}{\left(1 + bC_0\right)} \tag{8}$$

where C_0 is the initial concentration of analytes. If $R_L < 1$, then the adsorption is favorable, while if $R_L > 1$ indicates unfavorable adsorption. However, $R_L = 1$ and $R_L = 0$ indicate linear adsorption and irreversible adsorption, respectively [51,59].

The Langmuir isotherm model resulted in a good fit of experimental adsorption (exchange) data (Figs. 4a and b), which indicate that the model is appropriate for the

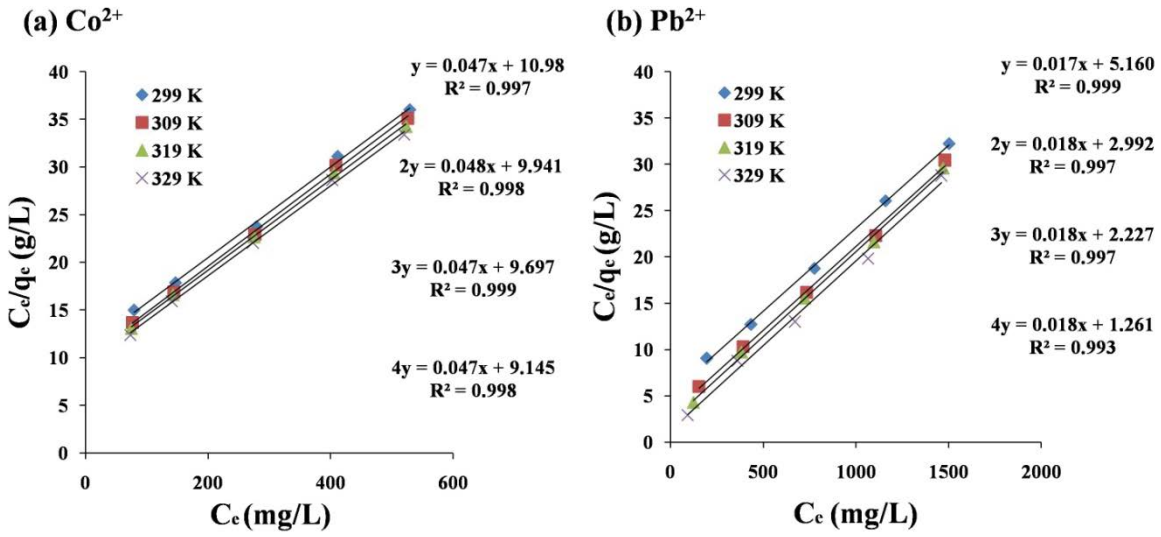

Fig. 4. Langmuir adsorption isotherms of (a) transition metal ion (Co^{2+}) and (b) heavy metal ion (Pb^{2+}): 299, 309, 319 and 329 K.

Table 6
Thermodynamic parameters evaluated for M^{2+}-H^{+} exchange at various temperatures using MCR

Metal ions	Temperature (K)	*K*	Δ*G*° (kJ/mol)	Δ*H*° (kJ/mol)	Δ*S*° (J/mol/°C)
Co^{2+}-H^{+}	299	2.14	–0.94	22.33	77.85
	309	2.18	–1.00		75.52
	319	2.25	–1.08		73.39
	329	2.32	–1.15		71.38
Ni^{2+}-H^{+}	299	1.96	–0.83	15.77	55.54
	309	1.98	–0.88		53.89
	319	2.05	–0.95		52.42
	329	2.07	–1.00		50.97
Cu^{2+}-H^{+}	299	2.28	–1.02	34.22	117.88
	309	2.45	–1.15		114.48
	319	2.49	–1.21		111.08
	329	2.59	–1.30		107.99
Zn^{2+}-H^{+}	299	2.11	–0.93	25.06	86.93
	309	2.23	–1.03		84.44
	319	2.24	–1.06		81.91
	329	2.33	–1.15		79.68
Cd^{2+}-H^{+}	299	2.00	–0.86	25.97	89.78
	309	2.09	–0.95		87.14
	319	2.18	–1.03		84.67
	329	2.21	–1.08		82.26
Hg^{2+}-H^{+}	299	2.27	–1.02	17.64	62.41
	309	2.29	–1.06		60.54
	319	2.39	–1.15		58.93
	329	2.42	–1.21		57.30
Pb^{2+}-H^{+}	299	2.19	–0.97	36.85	126.52
	309	2.28	–1.06		122.70
	319	2.42	–1.17		119.22
	329	2.51	–1.26		115.85

sorption of all of the metal ions under study. Further, lower b values again confirm that the adsorption is favorable. V_m (maximum metal ion adsorption capacity of the exchanger), follows the order $Zn^{2+} > Ni^{2+} > Co^{2+} > Cu^{2+}$ among transition metal ions and $Pb^{2+} > Cd^{2+} > Hg^{2+}$ among heavy metal ions.

3.5. Thermodynamic study of metal ion exchange process

In order to determine the basic thermodynamic parameters such as equilibrium constant (K), standard Gibbs free energy ($\Delta G°$), standard enthalpy ($\Delta H°$) and standard entropy ($\Delta S°$) changes, exchange was studied at different temperatures (299–329 K). Thermodynamic parameters are used to support the nature of the adsorption process proposed above. The calculated values of thermodynamic parameters are given in Table 6.

Further, equilibrium studies for metal-loaded MCR were apparently attained within 120 min. A plot between (Fig. 5) fractional attainment of equilibrium, $U(t)$ vs. time (t) gives idea of equilibrium saturation for each metal ion.

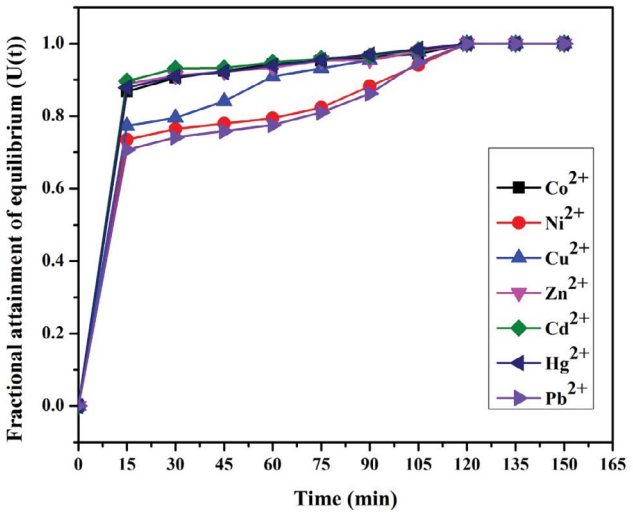

Fig. 5. Fractional attainment of equilibrium for varying metal ions vs. time using MCR.

K increases with increasing temperature for transition and heavy metal ions. This indicates higher affinity of metal ion to the exchanger at higher temperature, which reveals endothermicity of ion exchange process. The value of $\Delta G°$ is negative and decrease with increase in temperature. The negative $\Delta G°$ value means that all metal ion sorption onto the MCR and process favored with increasing temperature. This confirms that exchange process is feasible and spontaneous in nature. At any given temperature, high negative $\Delta G°$ value for Cu^{2+} and Hg^{2+} indicate ease of exchange for these metal ions. The parameters are driven by hydration of metal ions (less $\Delta G°$ values is related to more hydrated metal ion and vice versa). $\Delta H°$ was positive in all cases, indicating that the process is endothermic in nature. The order of enthalpy change for transition metal ions ($Cu^{2+} > Zn^{2+} > Co^{2+} > Ni^{2+}$) and heavy metal ions ($Pb^{2+} > Cd^{2+} > Hg^{2+}$) can be related to hydrated ion size. Higher/positive values of $\Delta H°$ indicate more endothermicity of the exchange process and the requirement of more energy for dehydration. The higher $\Delta S°$ values for Cu^{2+} and Pb^{2+} attributed to greater dehydration (which indicates greater disorder produced) during the exchange [60].

3.6. Adsorption kinetics

The kinetics of the adsorption of various metal ions (transition and heavy metal) using MCR was studied by observing q_t at varied contact time (t). To investigate the adsorption process of the metal ion on MCR, the pseudo-first-order, pseudo-second-order, and intraparticle diffusion models were used (Eqs. (3)–(5); see Figs. 6a–c). Kinetic parameters are shown in Table 7. Fig. 6 shows typical kinetics of adsorption for Zn^{2+} and Cd^{2+} ions. It can be observed that the adsorption of metal ion onto MCR was rapid in the first 15 min and then reached an equilibrium gradually in 120 min. Analysis of data shows distant R^2 values from 1 suggesting that pseudo-first-order is not applicable. However pseudo-second-order equation results (Table 7) matching of q_e(cal) and q_e(exp) together with a good correlation coefficient (Zn^{2+} = 0.998 and Cd^{2+} = 0.999). This

Table 7
Kinetic parameters of metal ion adsorption onto MCR conditions: 0.1 g adsorbent over 0.002 M at optimum conditions of other variables

Models	Parameters	Co^{2+}	Ni^{2+}	Cu^{2+}	Zn^{2+}	Cd^{2+}	Hg^{2+}	Pb^{2+}
Pseudo-first-order	K_1	0.0161	0.0138	0.0253	0.0161	0.0161	0.0207	0.0138
	q_e (cal)	10.023	6.0117	4.2072	10.889	5.6104	3.9902	1.1402
	R^2	0.992	0.963	0.959	0.923	0.925	0.944	0.946
Pseudo-second-order	K_2	0.4152	0.1735	0.1845	0.4398	0.2415	0.1854	0.0241
	q_e (cal)	0.6321	0.4172	0.5917	0.5956	1.3193	1.3495	2.5575
	R^2	0.999	0.984	0.997	0.998	0.999	0.999	0.9810
Intraparticle diffusion	K_{id}	0.010	0.017	0.019	0.008	0.017	0.022	0.116
	C	0.504	0.195	0.348	0.485	1.105	1.076	1.037
	R^2	0.975	0.943	0.976	0.960	0.964	0.993	0.945
Experimental	q_e (exp)	0.624	0.398	0.558	0.588	1.303	1.323	2.403

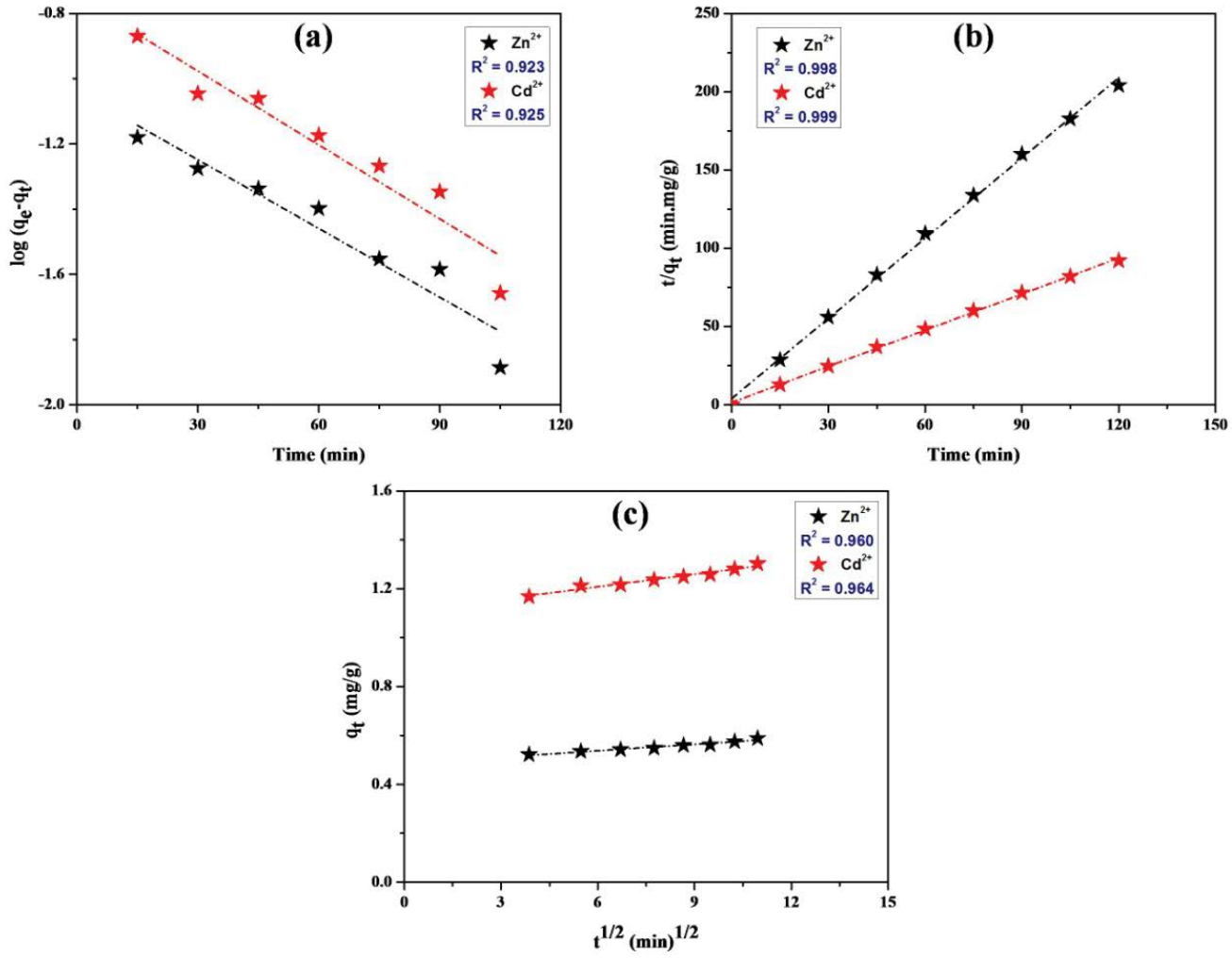

Fig. 6. (a) Pseudo-first-order kinetics, (b) pseudo-second-order kinetics and (c) intraparticle diffusion model for adsorption of transition metal (Zn^{2+}) and heavy metal ion (Cd^{2+}) on MCR.

suggests the validity of pseudo-second-order kinetics for adsorption process. All kinetic model graphs are shown in Figs. S8a–c and Figs. S9a–c.

The kinetic data were also evaluated by intraparticle diffusion Weber–Morris model. A plot of q_t vs. the square root of time ($t^{1/2}$) is linear if intraparticle diffusion is involved in the adsorption process. Further, such linear plots should pass through the origin. R^2 value (Zn^{2+} = 0.960 and Cd^{2+} = 0.964) and the absence of passing the straight line through the origin hint that the intraparticle diffusion model is not valid to explain present adsorption kinetics. On the basis of above discussion, adsorption of transition and heavy metal ion follows a pseudo-second-order reaction pathway [18,61].

3.7. Effect of nature of eluent

The elution behavior (Table 8) of transition and heavy metal ions (Co^{2+}, Ni^{2+}, Cu^{2+}, Zn^{2+}, Cd^{2+}, Hg^{2+} and Pb^{2+}) have been performed using different electrolytes (ammonium nitrate, perchloric acid, glacial acetic acid, and nitric acid). Eluent data of Table 8 shows that 0.2 M HNO_3 is a better eluent among others. Using 0.2 M HNO_3, order of the percentages of metal eluted among the transition metal ions was $Co^{2+} > Cu^{2+} > Ni^{2+} > Zn^{2+}$ and that among the heavy metal ions was $Hg^{2+} > Cd^{2+} > Pb^{2+}$. The % metal eluted in all cases is in the range of 60%–96%. K_d value indicate that Co^{2+} and Hg^{2+} metal ion exchanges more and hence less eluted as shown in Fig. 7 (for Co^{2+}) [62].

4. Conclusions

Amberlite IRA-400(Cl^-) resin has been modified (MCR) with disodium salt of EDTA. The MCR has been characterized by FTIR, EDX and SEM analysis and then used for the removal of metal ions from aqueous solution. Distribution coefficient (K_d) has been determined in aqueous or electrolytic solution for metal ion exchange. K_d values, at different time interval are used to evaluate fractional attainment of equilibrium. Effect of pH and nature of electrolyte has also been studied for the metal ion exchange process. The transition and heavy metal ions were adsorbed onto the MCR

Table 8
Percentage elution (%*E*) of metal ions in different electrolyte media using MCR

	Percentage elution (%*E*) of metal ions in different electrolyte media							
	NH_4NO_3		HNO_3		$HClO_4$		CH_3COOH	
Metal ions	0.02 M	0.2 M	0.02 M	0.2 M	0.02 M	0.2 M	0.02 M	0.2 M
Co^{2+}	62.47	69.41	81.83	91.62	69.41	70.80	69.41	76.35
Ni^{2+}	62.93	68.48	83.29	88.85	74.03	77.74	68.48	74.03
Cu^{2+}	67.16	70.28	82.78	90.60	79.66	85.91	71.85	78.10
Zn^{2+}	69.20	72.09	80.72	86.51	61.99	73.51	72.07	74.96
Cd^{2+}	60.30	63.00	90.35	91.77	68.36	75.30	79.47	82.16
Hg^{2+}	60.00	64.00	92.00	96.00	70.00	74.00	84.00	88.00
Pb^{2+}	61.22	63.02	88.23	90.03	70.24	72.02	77.43	81.04

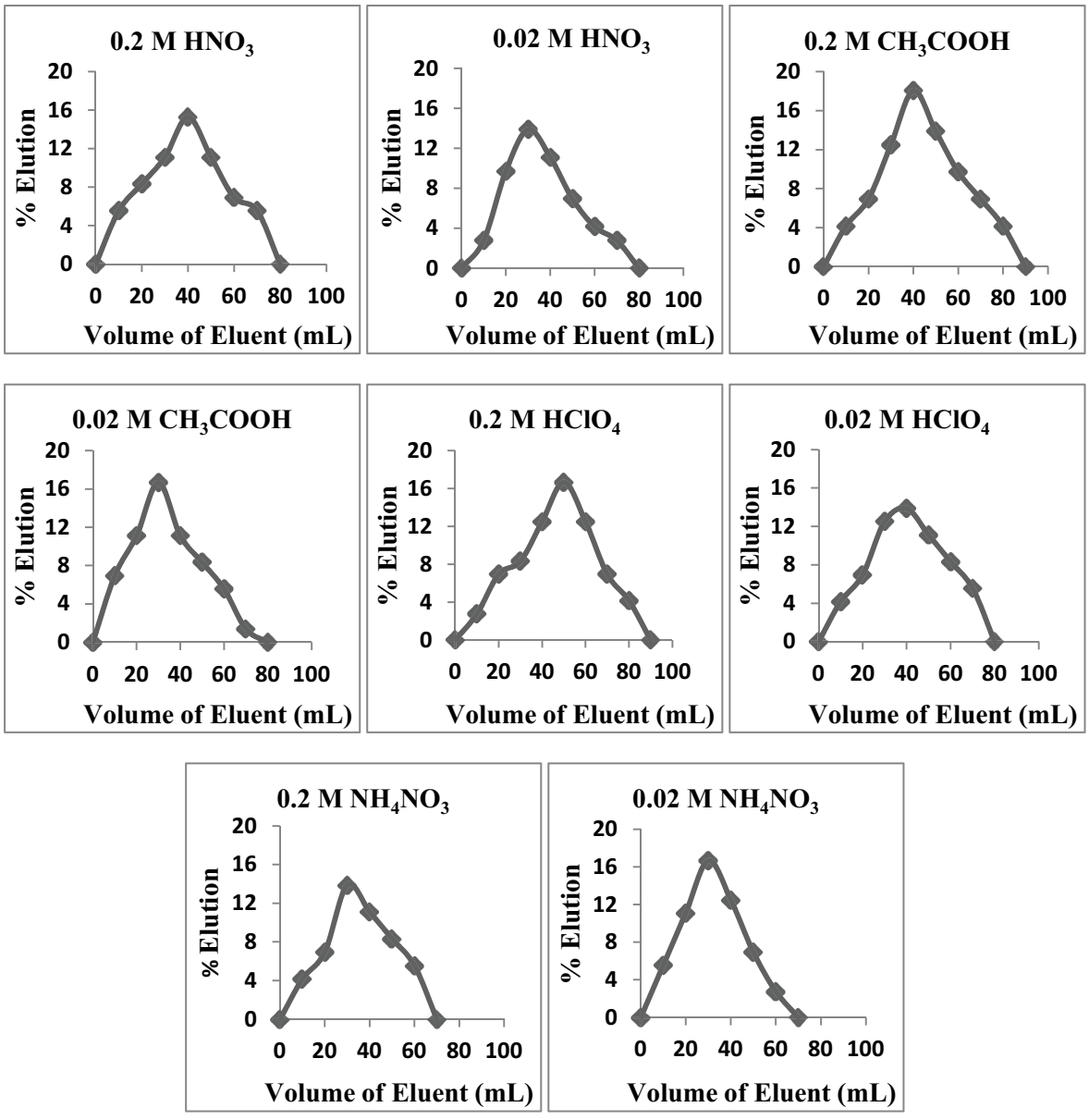

Fig. 7. Elution curve of Co^{2+} using MCR.

in a monolayer of adsorption as confirmed by applying Langmuir model. The adsorption mechanism of transition metal ion (Cu^{2+}) and heavy metal ion (Pb^{2+}) onto the MCR has been found endothermic as indicated from the higher positive value of $\Delta H°$. The higher negative value of $\Delta G°$ and positive value of $\Delta S°$ indicates the spontaneity of the metal ion exchange process. Adsorption data, with time, have been fitted well in pseudo-second-order kinetic model. Metal ion exchange process, developed have by using MCR, can be more effective than the other methods reported in the literature [51,56,57].

Acknowledgments

S.N. Katariya is thankful to Council for Scientific and Industrial Research (CSIR), New Delhi, India, for awarding junior research fellowship under grant [09/114(0229)/2019-EMR-I]. The authors would like to thank Head, Applied Chemistry Department, Faculty of Technology and Engineering, The Maharaja Sayajirao University of Baroda, for his kind support and for providing necessary facilities to carry out this work. The authors are also thankful to the Head, Department of Metallurgical and Materials Engineering, Faculty of Technology and Engineering for providing EDX analysis.

Symbols

K_d — Distribution coefficient
q_e — Amount of solute adsorbed of sorbent at equilibrium
q_t — Amount of solute on the surface of the adsorbent at time t.
K_1 — Pseudo-first-order rate constant
K_2 — Pseudo-second-order rate constant
K_{id} — Intraparticle diffusion rate constant
$\%E$ — % of metal ion eluted
C_e — Amount of adsorbate adsorbed at the equilibrium concentration
X — Equilibrium concentration of adsorbate
M — Amount of adsorbent
B — Adsorption bond energy
V_m — Maximum monolayer adsorption capacity
R_L — Separation factor

References

[1] N.L. Nemerow, A. Dasgupta, Ind. And Hazard Waste Treat., Van Nostrand Reinhold, New York, 1991, pp. 378.
[2] G. Tchobanoglous, L.B. Franklin, Waste Water Engineering: Treatment, Disposal and Reuse, McGraw-Hill, Inc., New York, 1991.
[3] I. Ali, H.Y. Aboul-Enein, Chiral Pollutants: Distribution, Toxicity and Analysis by Chromatography and Capillary Electrophoresis, John Wiley & Sons, Chichester, UK, 2004.
[4] I. Ali, New generation adsorbents for water treatment, Chem. Rev., 112 (2012) 5073–5091.
[5] A.M. Elbedwehy, A.M. Abou-Elanwar, A.O. Ezzat, A.M. Atta, Super effective removal of toxic metals water pollutants using multi functionalized polyacrylonitrile and arabicgum grafts, Polymers, 11 (2019) 1938.
[6] R. Kumar, S.K. Jain, R.K. Misra, M. Kachchwaha, P.K. Khatri, Aqueous heavy metals removal by adsorption on β-diketone-functionalized styrene–Divinylbenzene copolymeric resin, Int. J. Environ. Sci. Technol., 9 (2012) 79–84.
[7] Mu. Naushad, Inorganic and composite ion exchange materials and their applications, Ion Exch. Lett., 2 (2009) 1–14.
[8] L. Wang, L. Yang, Y. Li, Y. Zhang, X. Ma, Z. Ye, Study on adsorption mechanism of Pb(II) and Cu(II) in aqueous solution using PS-EDTA resin, Chem. Eng. J., 163 (2010) 364–372.
[9] N.T. Abdel-Ghani, A.K. Hegazy, G.A. El-Chaghaby, Typhadomingensis leaf powder for decontamination of aluminium, iron, zinc and lead: biosorption kinetics and equilibrium modeling, Int. J. Environ. Sci. Technol., 6 (2009) 243–248.
[10] J. Aguado, J.M. Arsuaga, A. Arencibia, M. Lindo, V. Gascon, Aqueous heavy metals removal by adsorption on amine functionalized mesoporous silica, J. Hazard. Mater., 163 (2009) 213–221.
[11] C.L. Ake, K. Mayura, H. Huebner, G.R. Bratton, T.D. Phillips, Development of porous clay-based composites for the sorption of lead from water, J. Toxicol. Environ. Health Part A, 63 (2001) 459–475.
[12] Z.A. ALOthman, Inamuddin, Mu. Naushad, Recent developments in the synthesis, characterization and applications of zirconium(IV) based composite ion exchangers, J. Inorg. Organomet. Polym., 23 (2013) 257–269.
[13] G. Zhou, J. Luo, C. Liu, L. Chu, J. Crittenden, Efficient heavy metal removal from industrial melting effluent using fixed-bed process based on porous hydrogel adsorbents, Water Res., 131 (2018) 246–254.
[14] L.T. Friberg, G.F. Nordberg, B.A. Fowler, M. Nordberg, Handbook on the Toxicology of metals, Elsevier, Amsterdam, The Netherlands, 1979.
[15] M. Devi, M. Fingermann, Inhibition of acetyl cholinesterase activity in the central nervous system of the redswamp crayfish, procambarus clarkia, by mercury, cadmium and lead, Bullet. Environ. Cont. Toxic., 55 (1995) 746–750.
[16] S.S. Kalaivani, V. Thangaraj, M. Arukkani, V.T. Kadathur, A. Dhanasekaran, S. Sivanesan, L. Ravikumar, The use of new modified poly(acrylamide) chelating resin with pendent benzo thiazole groups containing donor atoms in the removal of heavy metal ions from aqueous solutions, Water Res. Ind., 5 (2014) 21–35.
[17] R. Kumar, M.A. Barakat, Y.A. Daza, H.L. Woodcock, J.N. Kuhn, EDTA functionalized silica for removal of Cu(II), Zn(II), and Ni(II) from aqueous solution, J. Colloid. Int. Sci., 408 (2013) 200–205.
[18] I.M. Ali, M.Y. Nassar, Y.H. Kotp, M. Khalil, Cylindrical-design, dehydration and sorption properties of easily synthesized magnesium phospho-silicate nanopowder, Part. Sci. Technol., 37 (2019) 207–219.
[19] Y.H. Kotp, Enhancement of industrial effluents quality by using nanocomposite Mg/Al LDH ultrafiltration mambranes, J. Inorg. Organomet. Polym. Mater., 30 (2020) 5244–5260.
[20] Y.H. Kotp, High-flux TFN nanofiltration membranes incorporated with camphor-Al_2O_3 nanoparticles for brackish water desalination, Chemosphere, 265 (2021) 128999.
[21] A. Dabrowski, Z. Hubicki, P. Podkos'cielny, E. Robens, Selective removal of the heavy metal ions from waters and industrial waste waters by ion exchange method, Chemosphere, 56 (2004) 91–106.
[22] C. Mbareck, Q.T. Nguyen, O.T. Alaoui, D. Barillier, Elaboration, characterization and application of polysulfone and polyacrylic acid blends us ultrafiltration membranes for removal of some heavy metals from water, J. Hazard. Mater., 171 (2009) 93–101.
[23] S. Singh, P. Patel, V.K. Shahi, U. Chudasama, Pb^{2+} Selective and highly cross-linked zirconium phosphonate membrane by sol–gel in aqueous media for electrochemical applications, Desalination, 276 (2011) 175–183.
[24] M.E. Mahmoud, A.A. Yakout, H. Abdel-Aal, M.M. Osman, High performance SiO_2 nanoparticles-immobilized-penicillium funiculosum for bioaccumulation and solid phase extraction of lead, Bio. Res. Technol., 106 (2012) 125–132.
[25] M. Mohamed, E. Soliman, A. Dlssouky, Metal uptake properties of polystyrene resin immobilized polyamine and formyl salicylic acid derivatives as chelation ion exchangers, Analyt. Sci., 13 (1997) 765–769.

[26] C.F. Carolin, P.S. Kumar, A. Saravanan, G.J. Joshiba, Mu. Naushad, Efficient techniques for the removal of toxic heavy metals from aquatic environment: a review, J. Environ. Chem. Eng., 5 (2017) 2782–2799.
[27] Mu. Naushad, Surfactant assisted nano-composite cation exchanger: development, characterization and applications for the removal of toxic Pb^{2+} from aqueous medium, Chem. Eng. J., 235 (2014) 100–108.
[28] Mu. Naushad, Z.A. ALOthman, Separation of toxic Pb^{2+} metal from aqueous solution using strongly acidic cation-exchange resin: Analytical applications for the removal of metal ion from pharmaceutical formulation, Desal. Wat. Treat., 53 (2015) 2158–2166.
[29] C.K. Anh, D. Park, S.H. Woo, J.M. Park, Removal of cationic heavy metal from aqueous solution by activated carbon impregnated with anionic surfactants, J. Hazard. Mater., 164 (2009) 1130–1136.
[30] S. Zhang, X. Li, J.P. Chen, Preparation and evaluation of a magnetite doped activated carbon fiber for enhanced arsenic removal, Carbon, 48 (2010) 60–67.
[31] P.C. Mishra, R.K. Patel, Removal of lead and zinc from water by low cost adsorbents, J. Hazard. Mater., 168 (2009) 319–325.
[32] E.S. Dragan, M.V. Dinu, D. Timpu, Preparation and characterization of novel composites based on chitosan and clinoptilolite with enhanced adsorption properties for Cu^{2+}, Bio. Res. Technol., 101 (2010) 812–817.
[33] X. Wang, Y. Zheng, A. Wang, Fast removal of copper ions from aqueous solution by chitosan-g-poly(acrylic acid)/attapulgite Composites, J. Hazard. Mater., 168 (2009) 970–977.
[34] W. Peng, H. Li, Y. Liu, S. Song, A review on heavy metal ions adsorption from water by graphene oxide and its composites, J. Mol. Liq., 230 (2017) 496–504.
[35] T.G. Kebede, S. Dube, M.M. Nind, Bioremediation of Cd(II), Pb(II) and Cu(II) from industrial effluents by moringa stenopetala seed husk, J. Environ. Sci. Health, Part A, 54 (2019) 337–351.
[36] W. Shen, S. Chen, S. Shi, X. Li, X. Zhang, W. Hu, H. Wang, Adsorption of Cu(II) and Pb(II) onto diethylenetriamine-bacterial cellulose, Carbohydr. Poly., 75 (2009) 110–114.
[37] Y. Jiang, H. Pang, B. Liao, Removal of copper (II) ions from aqueous solution by modified bagasse, J. Hazard. Mater., 164 (2009) 1–9.
[38] G. Zhang, R. Qu, C. Sun, C. Ji, H. Chen, C. Wang, Y. Niu, Adsorption of metal ions of chitosan coated cotton fiber, J. App. Poly. Sci., 110 (2008) 2321–2327.
[39] B. Shah, U. Chudasama, Kinetics, thermodynamics and metal separation studies of transition (Co^{2+}, Ni^{2+}, Cu^{2+}, Zn^{2+}) and heavy metal ions (Cd^{2+}, Hg^{2+}, Pb^{2+}) using novel hybrid ion exchanger—Zirconium amino trismethylene phosphonic acid, Sep. Sci. Technol., 54 (2019) 1560–1572.
[40] S. Sun, A. Wang, Adsorption properties of N-succinyl-chitosan and cross linked N-succinyl-chitosan resin with Pb(II) as template Ions, Sep. Purif. Technol., 51 (2006) 409–415.
[41] P.A. Kavaklı, O. Güven, Removal of concentrated heavy metal ions from aqueous solutions using polymers with eriched amidoxime groups, J. Appl. Poly. Sci., 93 (2004) 1705–1710.
[42] J.N. Mathur, P.K. Khopkar, Solvent Extraction, Ion. Exch. Lett., 3 (1985) 653.
[43] S. Kocaoba, Comparison of Amberlite IR 120 and dolomite's performances for removal of heavy metals, J. Hazard. Mater., 147 (2007) 488–496.
[44] S. Kocaoba, Behaviour of cadmium(II) ions on cation-exchange resins, Adsorpt. Sci. Technol., 21 (2003) 831–840.
[45] M.A. Ali, M.A. Rahman, A.M. Shafiqul Alam, Use of EDTA-grafted anion – exchange resin for the separation of selective heavy metal ions. Anal. Chem. Lett., 3 (2013) 199–207.
[46] P. Kampalanonwat, P. Supaphol, Preparation and adsorption behavior of aminated electrospun polyacrylonitrile nano fiber mats for heavy metal ion removal, Appl. Mater. Interfaces, 2 (2010) 3619–3627.
[47] B.L. Rivas, S. Villegas, B. Ruf, Water insoluble polymers containing amine, sulfonic acid, and carboxylic acid groups: synthesis, characterization, and metal-ion-retention properties, J. Appl. Poly. Sci., 99 (2006) 3266–3274.
[48] O.G. Marambio, D.C. Pizarro, M. Jeria-Orell, M. Huerta, C. Olea-Azar, W.D. Habicher, Poly (N-phenylmaleimide-co-acrylicacid)–Copper(II) and poly (N-phenylmaleimide-co-acrylicacid)-cobalt(II) complexes: synthesis, characterization, and thermal behavior, J. Poly. Sci. Part A, 43 (2005) 4933–4941.
[49] C. Liu, R. Bai, L. Hong, Diethylenetriamine-grafted poly(glycidylmethacrylate) adsorbent for effective copper ion adsorption, J. Colloid Interface Sci., 303 (2006) 99–108.
[50] P. Patel, U. Chudasama, Synthesis and characterization of a novel hybrid cation exchange material and its application in metal ion separations, Ion. Exch. Lett., 4 (2011) 7–15.
[51] T. Parangi, B. Wani, U. Chudasama, Sorption and separation study of heavy metal ions using cerium phosphate: a cation exchanger, Desal. Wat. Treat., 57 (2015) 1–9.
[52] S. Nethaji, A. Sivasamy, A.B. Mandal, Adsorption isotherms, kinetics, and mechanism for the adsorption of cationic and anionic dyes onto carbonaceous particles prepared from juglans regia shell biomass, Int. J. Environ. Sci. Technol., 10 (2013) 231–242.
[53] S. Lagergren, About the theory of so-called adsorption of soluble substances, Kungligasvenskavet enskapsakademiens. Handl. Band., 24 (1898) 1–39.
[54] Y.S. Ho, G. McKay, Pseudo-second-order model for sorption processes, J. Proc. Biochem., 34 (1999) 451–465.
[55] W.J. Weber, J.C. Morris, Adsorption Processes for Water Treatment, Butterworth, London, 1987.
[56] T. Parangi, B. Wani, U. Chudasama, Synthesis, characterization and application of cerium phosphate as an ion exchanger, Desal. Wat. Treat., 38 (2012) 126–134.
[57] R. Saravanan, R. Mahalakshmi, M.S. Karthikeyan, L. Ravikumar, Chelating modified cellulose bearing pendant heterocyclic moiety for effective removal of heavy metals, Water Sci. Technol., 80 (2019) 1549–1561.
[58] S. Xiuling, D. Huipu, S. Liu, Q. Hui, Adsorption properties of Ni(II) by D301R anion exchange resin, J. Chem., 2014 (2014) 5.
[59] W. Li, Q. Liu, J. Liu, H. Zhang, R. Li, Z. Li, X. Jing, J. Wang, Removal U (VI) from artificial seawater using facilely and covalently grafted polyacrylonitrile fibres with lysine, Appl. Surf. Sci., 403 (2017) 378–388.
[60] R. Kunin, Ion Exchange Resin, J. Am. Pharm. Assoc., 47 (1958) 836.
[61] S. Sinha, S.S. Behera, S. Das, A. Basu, R.K. Mohapatra, B.M. Murmu, N.K. Dhal, S.K. Tripathy, P.K. Parhi, Removal of congo red dye from aqueous solution using amberlite IRA-400 in batch and fixed bed reactors, Chem. Eng. Commun., 205 (2018) 2–12.
[62] P. Patel, U. Chudasama, Application of a novel hybrid cation exchange material in metal ion separations, Sep. Sci. Technol., 46 (2011) 1346–1347.

Supplementary information

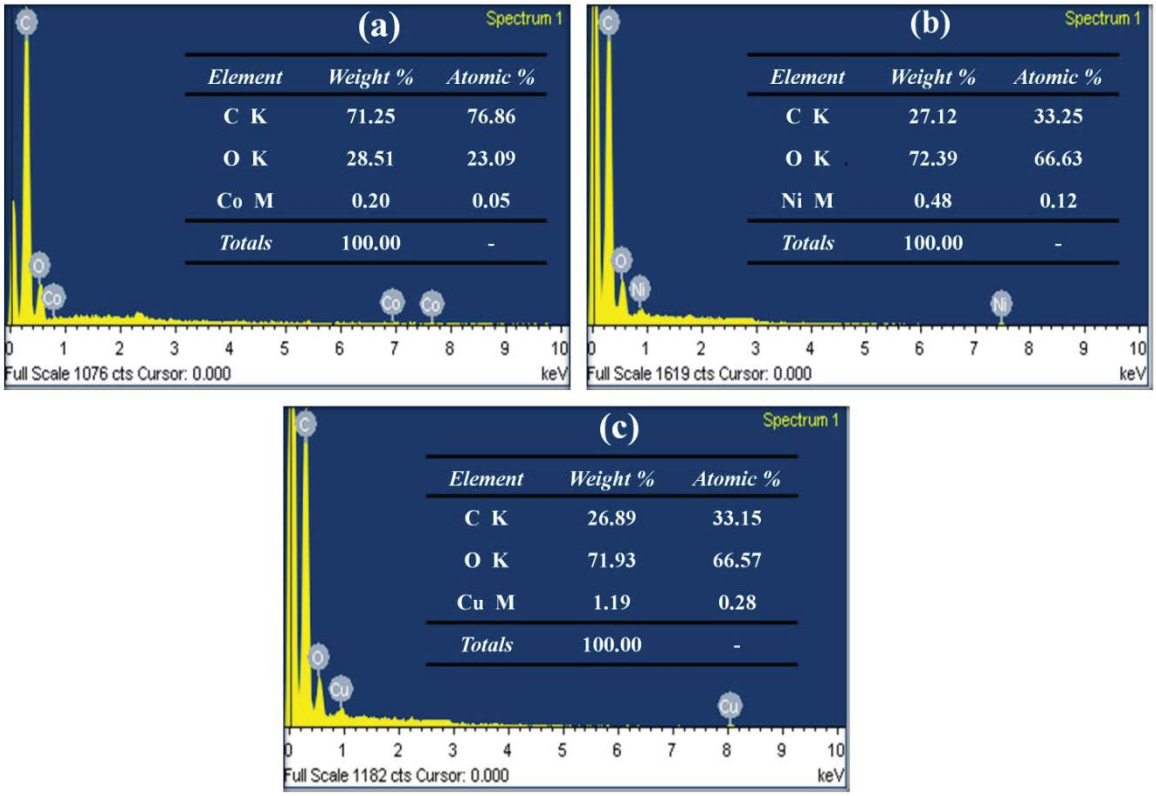

Fig. S1. EDX spectra of (a) Co^{2+}, (b) Ni^{2+}, and (c) Cu^{2+} loaded MCR.

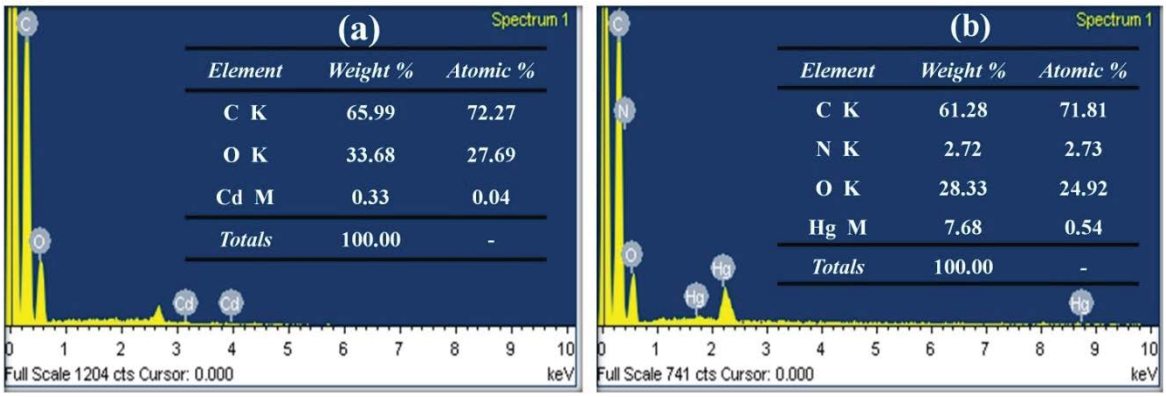

Fig. S2. EDX spectra of (a) Cd^{2+} and (b) Hg^{2+} loaded MCR.

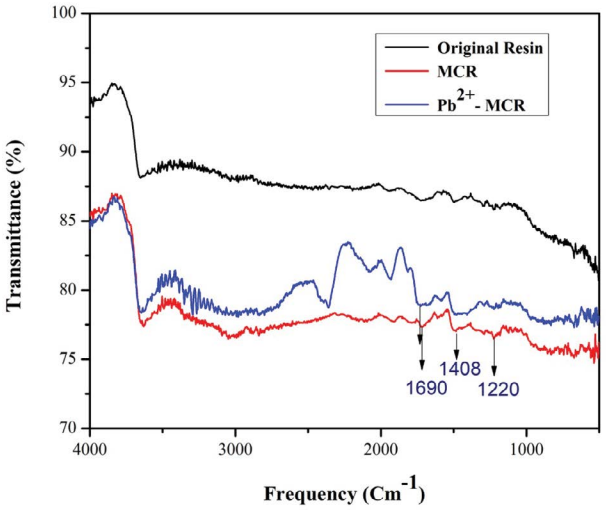

Fig. S3. FTIR of Amberlite IRA-400(Cl^-) resin (Original resin), MCR, and Pb^{2+} loaded MCR.

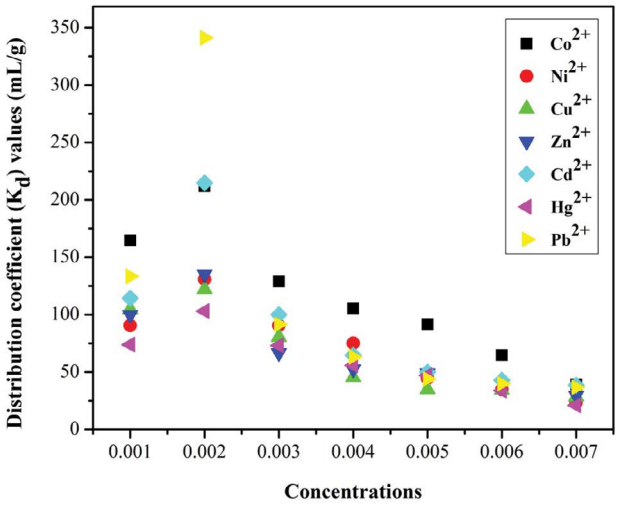

Fig. S4. Effect of metal ion Co^{2+}, Ni^{2+}, Cu^{2+}, Zn^{2+}, Cd^{2+}, Hg^{2+} and Pb^{2+} for concentration vs. distribution coefficient (K_d) value.

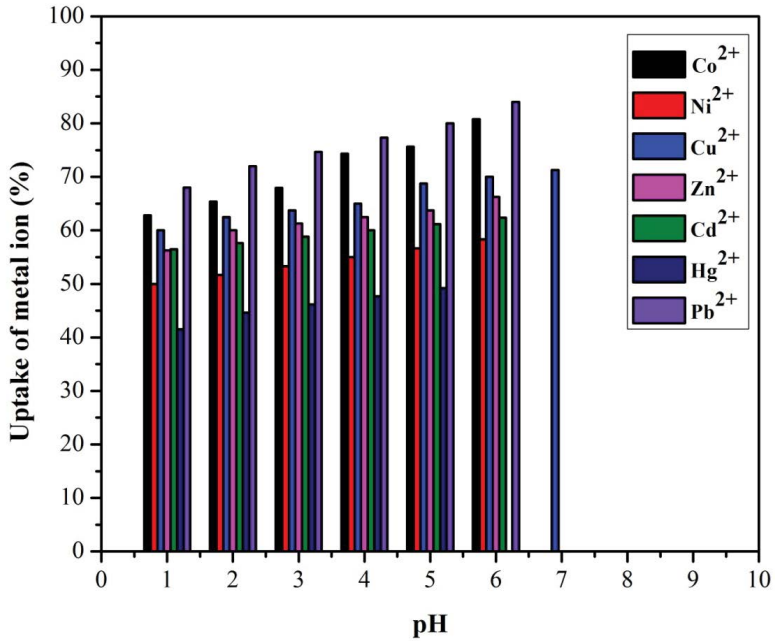

Fig. S5. % Uptake of Co^{2+}, Ni^{2+}, Cu^{2+}, Zn^{2+}, Cd^{2+}, Hg^{2+} and Pb^{2+} metal ions vs. pH.

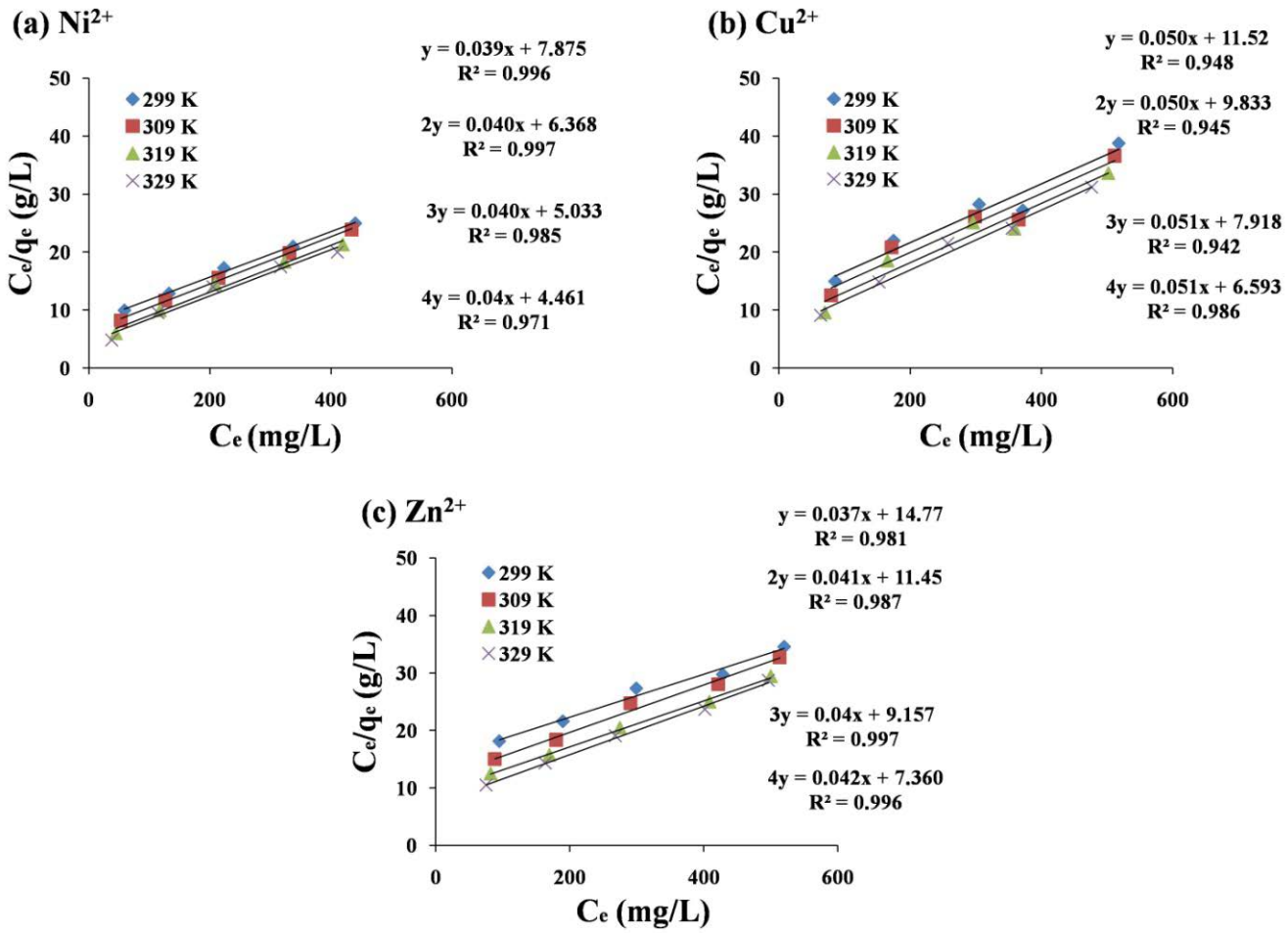

Fig. S6. Langmuir adsorption isotherms of transition metal ions (a) Ni^{2+}, (b) Cu^{2+} and (c) Zn^{2+}: 299, 309, 319 and 329 K.

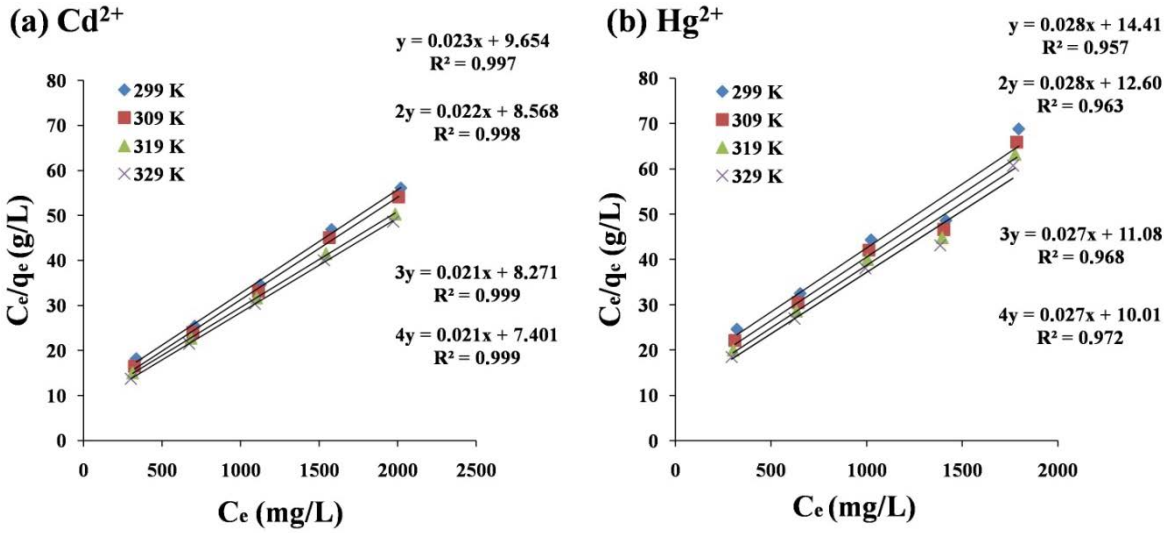

Fig. S7. Langmuir adsorption isotherms of transition metal ions (a) Cd^{2+} and (b) Hg^{2+}: 299, 309, 319 and 329 K.

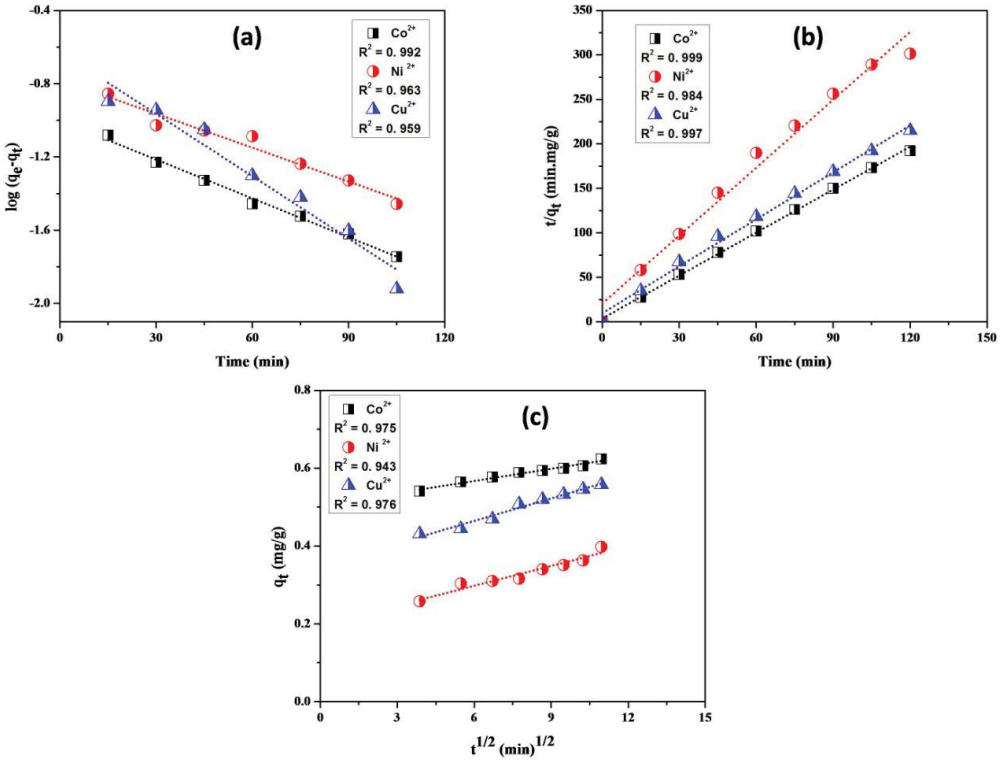

Fig. S8. (a) Pseudo-first-order kinetics, (b) Pseudo-second-order kinetics, and (c) intraparticle diffusion model for adsorption of transition metal (Co^{2+}, Ni^{2+}, Cu^{2+}) on MCR.

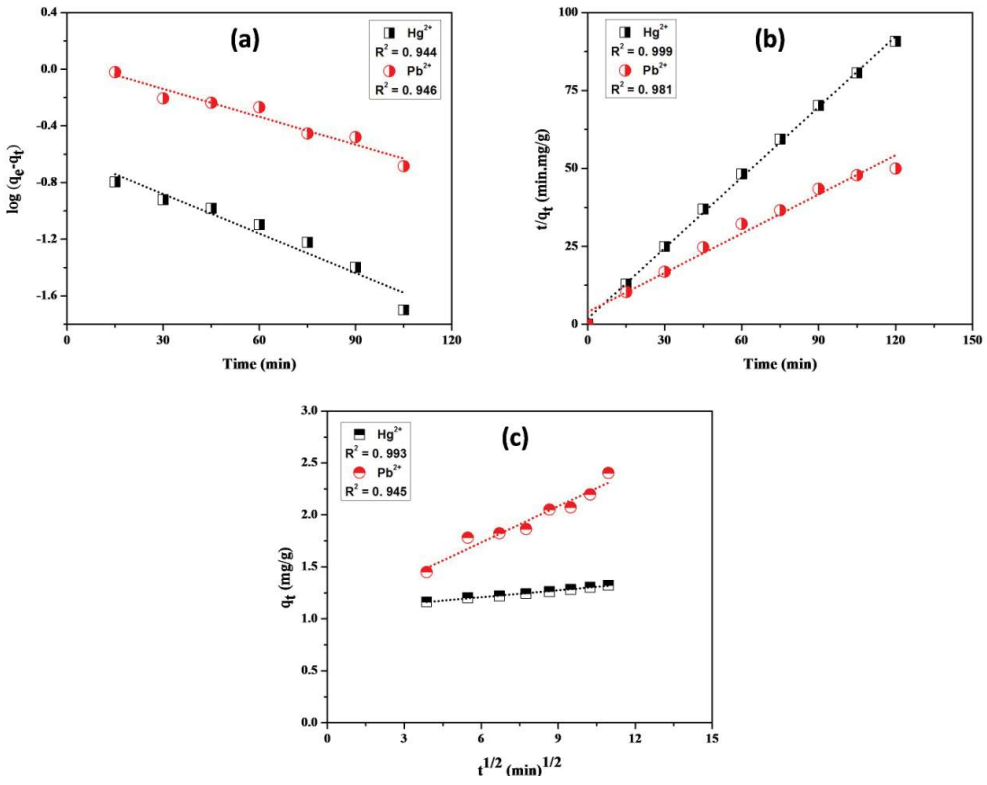

Fig. S9. (a) Pseudo-first-order kinetics, (b) Pseudo-second-order kinetics, and (c) intraparticle diffusion model for adsorption of heavy metal (Hg^{2+} and Pb^{2+}) on MCR.